IEEE Access
Multidisciplinary · Rapid Review · Open Access Journal

SPECIAL SECTION ON 74NETWORKS OF UNMANNED AERIAL VEHICLES: WIRELESS COMMUNICATIONS, APPLICATIONS, CONTROL AND MODELLING

INVITED PAPER

Flying Drone Base Stations for Macro Hotspots

AZADE FOTOUHI [1,2], **MING DING** [2], (Senior Member, IEEE), AND
MAHBUB HASSAN [1], (Senior Member, IEEE)

[1] University of New South Wales (UNSW), Sydney, NSW 2052, Australia
[2] CSIRO DATA61, Alexandria, NSW 1435, Australia

Corresponding author: Azade Fotouhi (azade.fotouhi@data61.csiro.au)

ABSTRACT We study a scenario where multiple drone-mounted base stations cruise freely over a macro hotspot to serve mobile users on the ground. The drone base stations move constantly and update their moving directions following our proposed mobility control algorithm. The constant movement of drones reduces the distance between the base stations and users, which in turn improves the probability of having a line of sight connection. We consider a practical user association scheme for the moving base stations, which enables user equipments to switch their serving base stations based only on the received signal strength. via extensive simulations, we demonstrate that the drone base stations moving according to our proposed algorithms can improve the average packet throughput by 82% and the 5th-percentile packet throughput by 430% compared to a baseline scenario, where drones hover over fixed locations. These improvements can be realized regardless of users' and base stations' density. The constant movement of the drones also helps reduce the total number of drones required to cover the macro hotspot.

INDEX TERMS Unmanned aerial vehicles, Drone base station, mobility control, game theory, network optimization.

I. INTRODUCTION

Due to their ability to autonomously move to any hard-to-reach-areas, drones or small unmanned aerial vehicles (UAVs) are becoming a promising solution for a wide range of applications in cellular networks. For example, drones equipped with light-weight base station (BS) hardware can act as a flying BS, creating an attractive alternative to conventional roof-top or pole-mounted BSs. In our research, we are leveraging the flexibility and agility of drones to study a new breed of drone BSs (DBSs) that can move continuously over the serving area. Such DBSs can continuously adapt their moving directions in order to provide higher service quality for mobile users on the ground.

In this paper, we focus on a practical scenario, where drones provide emergency coverage to a large area struck by disasters that destroyed all or most of the existing cell towers in the area. In this case, users can move around in the entire area. We refer to such areas as macro-hotspots due to the larger size of the area compared with conventional pico-hotspots. For such macro-hotspots, it is more meaningful for drones to fly over the entire area to serve as many users as they can, instead of limiting themselves in pre-defined small areas. In this scenario, the following challenges arise:

- Due to the free movement of DBSs over the entire service area, a user may frequently find different DBSs

available for communication. Therefore, users should be able to re-select their serving DBS in the network area.
- The probability of physical collision between DBSs arises, as they are assumed to be deployed at the same optimal altitude and can move around the entire network freely.
- By allowing DBSs to move freely over the entire service area, it is necessary to optimize the number of DBSs to achieve a certain performance target at a minimum cost.

In this paper, we address all of the above mentioned challenges. Our contributions can be summarized as follows:

- We propose a game theoretic distributed mobility control algorithm to guide the movement of the drones in the service area. We demonstrate that the proposed mobility control can not only optimize the spectral efficiency of the system, but also reduce the number of required drones in the network. We also show that the proposed mobility algorithm helps to prevent drones flying too close to each other, which reduces the risk of collisions
- We propose a simple and practically realizable user association scheme for the moving DBSs, which makes association decisions based only on the received signal strength.
- Using extensive simulations, we show that our proposed user association and drone mobility control algorithms

can improve the average packet throughput by 82% and the 5th-percentile packet throughput by 430% compared to the baseline scenario, where drones hover over fixed locations. These improvements can be realized regardless of users' and base stations' density.

The rest of this paper is structured as follows. The related work is reviewed in Section II. The system model is presented in Section III, followed by performance metrics in Section IV. We then explain our proposed drone movement algorithm in Section V. In Section VI, the simulation results are presented. Finally, our conclusions are drawn in Section VII.

II. RELATED WORK

In this section, we review the recent drone-related research relevant to cellular networks.

Due to special characteristics of UAVs and drones [1], finding a realistic and reliable path loss and fading models is one of the basic challenges in drone communications. Several studies demonstrate that a model that depends on the altitude and the elevation angle of UAVs fits the best for drone communications [2]–[4]. The proposed model is validated by experiments and used in our work as well.

Additionally, due to the flexibility and mobility of drones, authors employed them in different approaches. Deploying one single drone at fixed altitude hovering above the target area is addressed in [2] and [5]. It is shown that there is an optimal altitude for one UAV to provide the maximum coverage of the area. Another recent study by Mozaffari *et al.* [6] involves finding the optimal cell boundaries and deployment locations for multiple non-interfering UAVs. The objective of this study is to minimize the total transmission power of UAVs. Moreover, Bor-Yaliniz *et al.* [7] discussed finding the 3D optimal location for deploying a drone cell to provide services for the maximum number of users satisfying their SNR (Signal to Noise Ratio) constraints.

Rather than deploying UAVs in optimal location, dynamic movement of UAVs are also investigated in the literature. Following a predefined path, specially circular trajectory, is one of the common mobility models for drones, addressed in [8] and [9]. The center and the radius of circular path are adjusted for better performance between ground users and the UAV. Irregular movement is another way to gain benefits of drone's abilities [10]–[12]. Motion control of UAVs' chain to improve the link capacity between two mobile nodes is explored in [10]. Artificial Potential Field model is used to control the speed and heading angle of UAVs. A maximum turning angle and speed is defined for drones.

In our previous work [13], we designed drone mobility control algorithms according to drone's practical limitation [14], in order to improve the performance of the cellular network. DBS's mobility was limited to its small cell boundaries, and all users in the small cell were assumed to be associated to their local DBS all the time. we have shown that letting drones chasing users can significantly improve the system performance, especially the packet throughput for cell-edge users. In this work, we employ drones in a large area where they can move freely. Users are also allowed to move freely in the entire networks. Considering mobile users, multiple interfering drones, and practical limitations on drones' movements bring new challenges in this work. In the following section we review the system model and our proposed algorithm for DBSs.

III. SYSTEM MODEL

We assume there is a large network area with a size of $L(m) \times L(m)$, which will be covered by flying DBSs. There are U mobile users initially placed randomly in the serving area, moving according to the Random Way Point Model (RWP). In this model, each user selects a random destination within the area border independent of other users and moves there following a straight trajectory with a constant speed selected randomly from a given range. Upon reaching the destination, users may pause for a while before continuing to move to another destination [15]–[17]. Moreover, there are N DBSs, constantly moving in the network with a constant speed v (m/s), at a fixed altitude of h (m). Figure 1 illustrates the considered network scenario.
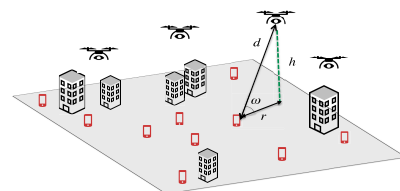

FIGURE 1. Considered network area with multiple mobile users and DBSs.

Note that, deploying drones at the same height with free movement would cause potential collision among drones. One alternative to avoid such collision issue is to use the height separation technique, i.e., deploying DBSs at various heights. However, by using height separation, drones could be deployed at a vast range of heights, causing performance degradation for the system. As a result, we assume all DBSs are flying at the same height and address the possibility of collision later.

DBSs may be connected to a nearby cell tower with wireless backhaul links. We further assume that each DBS is transmitting data to users using a fixed transmission power of p_{tx} (watt), a total bandwidth B (Hz) centered on a carrier frequency of f (Hz). It is assumed that transmissions from DBSs can create interference up to κ meters. The interference beyond κ meter is assumed to be negligible.

The *ground distance* or the two-dimensional (2D) distance between user u ($u \in [1, 2, \ldots, U]$), and drone n ($n \in [1, 2, \ldots, N]$) is defined by the distance between the user and the projection of the drone location onto the ground, denoted by $r_{u,n}$. The *euclidean distance* or the three-dimensional (3D) distance between user u and drone n is then presented by $d_{u,n} = \sqrt{r_{u,n}^2 + h^2}$, where h is the height of drone.

A. CHANNEL MODEL

In this paper, we consider a practical path loss model incorporating both LoS (Line of Sight), and NLoS (Non Line of Sight) transmissions. More specifically, the path loss function is formulated according to a probabilistic LoS model [2], [3], in which the probability of having a LoS connection between a drone and its user depends on the elevation angle of the transmission link. According to [2], the LoS probability function can be expressed as

$$P^{LoS}(u, n) = \frac{1}{1 + \alpha \times e^{(-\beta[\omega - \alpha])}}, \quad (1)$$

where α and β are environment-dependent constants, ω equals to $\arctan(h/r_{u,n})$ in degree. Although this model is recommended by 3GPP/ITU for urban scenarios, it would still be valid for disasters, as buildings will not be completely destroyed for most disasters. Moreover, the ratio of built-up land area to the total land can be changed by adjusting the environment-dependent parameters. As a result of (1), the probability of having a NLoS connection can be written as

$$P^{NLoS}(u, n) = 1 - P^{LoS}(u, n). \quad (2)$$

From (1) and (2), the path loss in dB can be modeled as

$$\eta_{path}(u, n) = A_{path} + 10\gamma_{path} \log_{10}(d_{u,n}), \quad (3)$$

where the string variable *"path"* takes the value of "LoS" and "NLoS" for the LoS and the NLoS cases, respectively. In addition, A_{path} is the path loss at the reference distance (1 meter) and γ_{path} is the path loss exponent, both obtainable from field tests [18].

B. TRAFFIC MODEL

The traffic model for each user follows the 3GPP recommendation [19]. In this model, there is a reading time interval between two subsequent user's data packet request. The reading time of each data packet is modeled as an exponential distribution with a mean of λ (sec). Moreover, the transmission time for each data packet is defined as the time interval between the request time of a data packet and the end of its download, denoted by τ (sec).

All data packets are assumed to have a fixed size of s (MByte). A user is referred to as an *active* user during the transmission time.

C. COMMUNICATION MODEL

The received signal power, $S^{path}(u, n)$ (watt), of an active user u associated with drone n can be expressed by

$$S^{path}(u, n) = \frac{b_u}{B} \times p_{tx} \times 10^{\frac{-\eta_{path}(u,n)}{10}} \quad (4)$$

where b_u ($0 \leq b_u \leq B$) is the allocated bandwidth to the user.

Moreover, the total noise power, N_u (watt), for an active user u including the thermal noise power and the user equipment noise figure, can be represented by [20]

$$N_u = 10^{\frac{-174 + \delta_{ue}}{10}} \times b_u \times 10^{-3}, \quad (5)$$

where δ_{ue} (dB) is the user equipment noise figure.

Accordingly, the *Signal to Noise (SNR)* and *Signal to Interference plus Noise Ratio (SINR)* of user u associated to drone n can be expressed by

$$SNR^{path}(u, n) = \frac{S^{path}(u, n)}{N_u}, \quad (6)$$

$$SINR^{path}(u, n) = \frac{S^{path}(u, n)}{I_u + N_u}, \quad (7)$$

where $I_u = \left(\sum_{i \in N, i \neq n, r_{u,i} \leq \kappa} S^{path}(u, i)\right)$ represents the interference signal from neighbor DBSs received by user u.

Then, the *spectral efficiency (SE)* (bps/Hz) of an active user u associated with drone n can be formulated according to the Shannon Capacity Theorem as [21]

$$\Phi^{path}(u, n) = \log_2(1 + SINR^{path}(u, n)). \quad (8)$$

Given the probabilistic channel model, the average SE for user u is given by

$$\bar{\Phi}(u, n) = P^{LoS} \times \Phi^{LoS}(u, n) + P^{NLoS} \times \Phi^{NLoS}(u, n). \quad (9)$$

Moreover, the *Throughput* (bps) of a communication link between an active user u and drone n can be formulated as

$$T(u, n) = b_u \times \bar{\Phi}(u, n). \quad (10)$$

D. DRONE MOBILITY CONTROL

Since all DBSs are flying at the same height, we consider their mobility in the 2D plane only. In more detail, we assume that each drone moves *continuously* in the 2D plane with a constant linear speed of v, and updates its moving direction every t_m sec, hereafter called *Direction Update Interval*. The proposed continuously moving model is thus applicable to all types of drones, with or without drone rotors.

When a drone wants to change its direction while keeping a constant speed, it moves along an arc. More importantly, the maximum possible turning angle θ_{max} for a drone during a specific time t_m can be obtained by $\theta_{max} = \frac{a_{max} \times t_m}{v}$, where a_{max} and v is the maximum centripetal acceleration and the speed of drone, respectively [14], [22]. At every t_m, the DBS chooses an angle, θ_n, between $\pm[0, \theta_{max}]$ and starts to complete the turn at the end of next t_m sec.

E. USER ASSOCIATION SCHEME

At any particular time, a set of users are connected to a DBS. However, when drones can move freely in the entire network area, users can reselect their serving DBSs frequently. The set of all active users associated to a DBS n at a specific time t is denoted by $Q_n(t)$ ($0 \leq |Q_n(t)| \leq U$). Additionally, the total bandwidth of B is shared *equally* among all associated active users of a DBS, and the DBS updates resource allocation every t_r second, which is referred to as *Resource Allocation Interval*.

In the considered user association scheme, a user selects a DBS with the highest received signal strength (RSS), and can reselect its serving DBS every t_r. There is no limitation on the number of users that can be associated to a specific DBS.

Note that each user can independently choose its serving DBS according to the observed RSS without any additional information from the other users.

IV. PERFORMANCE METRICS

In this section, we define the required metrics to evaluate the network performance.

A. PACKET THROUGHPUT

The *Packet Throughput*, the ratio of successfully transmitted bits over the time consumed to transmit the said data bits, can be expressed as

$$P = s \times \frac{1}{\tau}, \tag{11}$$

where s is the packet size, and τ is the transmission time. Recall that the transmission time for each data packet is defined as the time interval between the request time of a data packet and the end of its download. The traffic model for each user is shown in Figure 2.
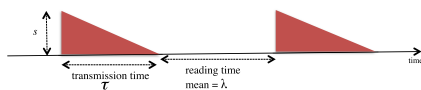

FIGURE 2. The traffic model per user.

B. 5TH-PERCENTILE PACKET THROUGHPUT

In order to evaluate the performance of DBSs for the cell edge users, the lowest 5th percentile of packet throughput is considered, as recommended by the 3GPP [23]. Generally speaking, a more homogeneous distribution of the user experience over the coverage area is highly desirable, and hence improving the cell edge performance is particularly useful for operators in practice.

C. USER-TO-DBS DISTANCE

One of the main motivation of mobile DBSs is to get close to users and shorten the distance between users and BSs. As a result, we investigate on the user-to-DBS ground distance to see the impact of drones mobility on it.

D. DBS-TO-DBS DISTANCE

In the free movement models, drones can fly over the entire network area, however keeping a safe distance to avoid physical collision between DBS is also very important. Moreover, maintaining a reasonable distance among DBSs can help to alleviate the interference problem.

E. PROBABILITY OF LOS

The probability of having a LoS connection between a serving DBS and an active user mainly depends on the height of the drone and the elevation angle of the transmission link. (See Equation 1) Higher LoS probability will improve the communication quality, results in higher network performance. Therefore, the probability of LoS is considered as one the performances metrics in this paper.

V. DBS MOBILITY ALGORITHM

In this paper, we propose a DBS mobility algorithms (DMAs) that employs Game Theory to make mobility decisions.

The task of a DMA is to choose turning angles for DBSs at the start of every t_m interval to improve the performance of the system. The DBS will continue to follow the path specified by the turning angle selected at the *start* of the interval for the next t_m seconds. This path cannot be changed in the middle of t_m despite any further changes in mobile user population and traffic in the system. When there is no associated user to a DBS, it chooses a random direction that keeps the drone in the intended border.

To reduce the complexity of the problem, we discretized all turning options into a finite set of $[-\theta_{max}, \ldots, -2g, -g, 0, g, 2g, \ldots, \theta_{max}]$, where $g = \frac{2\theta_{max}}{G-1}$, with G representing the total number of turning options. Each drone can choose its direction from G candidate ones.

In the game theory based DMA, the direction selection is formulated as a non-cooperative game played by all serving DBSs in the system. The game is played at the start of each t_m interval and the decisions leading to the Nash Equilibrium (NE) are adopted by the DBSs to update their directions. A pure NE is a convergence point where no player has an incentive to deviate from it by changing its action. Hereafter, we refer to this algorithm as *GT* DMA.

The game is described by $\mathcal{G} = (\mathcal{P}, \{\mathcal{A}_p\}, u_p)$, where $\mathcal{P} = \{1, 2, \ldots, P\}$ is the set of DBSs as players with at least one associated active user. $\mathcal{A}_p$ is the set of actions (G turning angles) for each DBS, and u_p is the utility function of each DBS.

Furthermore, $u_p : \mathcal{A} \rightarrow IR$ maps any member of the action space, $\theta \in \mathcal{A}$, to a numerical real number. The action space $\mathcal{A}$ is defined as the Cartesian product of the set of actions of all players ($\mathcal{A} = \mathcal{A}_1 \times \mathcal{A}_2 \times \cdots \times \mathcal{A}_P$). We denote the utility function of each player as $u_p(\theta_p, \theta_{-p})$, where θ_{-p} presents the action of all players except p. The utility function for each player is defined by the spectral efficiency of that player given the action of all players, as follows

$$u_p(\theta) = u_p(\theta_p, \theta_{-p}) = \bar{\Phi}(p), \tag{12}$$

where $\bar{\Phi}(p)$ is the average SE for the active users associated to DBS p.

In a non-cooperative game, each player independently tries to find an action that maximizes its own utility, however its decision is influenced by the action of other players:

$$\theta_n = \arg \max_{\forall \theta_p \in \mathcal{A}_p} u_p(\theta_p, \theta_{-p}) \quad \forall p \in \mathcal{P}. \tag{13}$$

In this algorithm, at first, all drones select a random direction from their set of actions. Then each of them finds their

best response considering other players' action that maximize the utility function. Exhaustive search is considered to find the best response. Finally, after few trials they all converge to a NE point and move towards the selected directions during the next t_m interval.

VI. SIMULATION AND DISCUSSION

In this section, the performance of the DBS network where both users and DBSs are free to move in the entire network area is evaluated through extensive simulations by MATLAB. In this model, the RSS-based user association scheme is employed. The numerical results are compared against those of non-moving DBSs, i.e., hovering over the serving area. Such baseline scheme is referred to as the hovering (*HOV*) model.

In the *HOV* model, the total network area is reformed into a regular grid of squares based on the number of available DBSs. Each DBS is deployed hovering at the target height above the centre of such squares. For example, given an area of size 560m × 560m, and 16 available DBSs, the area is divided into a 4×4 squares, each of size 140m × 140m. Then a DBS is deployed above the centre of each square.

The DBS' speed vary from 2m/s to 8m/s, with the capability of changing direction every $t_m = 1s$. Moreover, the current observed drone centripetal acceleration is set to 4 m/s^2 [24], while higher centripetal acceleration are expected for future drones.

The recommended height of 10m [25] is selected for all DBSs in our simulation. The number of users and their traffic model follow the parameters recommended by the 3GPP [19] shown in Table 1. Our preliminary simulation results show that the system performance becomes stable after 500 seconds. As a result, we run all simulations for 800 seconds to obtain meaningful results. Moreover, to mitigate the randomness of the results, all results have been averaged over 10 independent runs of 800-second simulations.

TABLE 1. Definition of parameters and their value.

Symbol	Definition	Value
N	Number of Drones	[144, 100, 49, 36, 25, 16]
B	Total Bandwidth	5 MHz
U	Number of Users	[245, 392, 490]
h	Drone Height	10 m
v	Drone Speed	[2, 4, 6, 8] m/s
L	Length of the Network Area	560m
f	Working Frequency	2 GHz
p_{tx}	Drone Transmission Power	24 dBm [18]
λ	Mean Reading Time	40 sec
α, β	Environmental Parameter for Urban Area	9.61 , 0.16 [7]
γ	Path Loss Exponent (LoS/NLoS)	2.09/3.75 [18]
δ_{ue}	UE Noise Figure	9 dB
t_m	Direction Update Interval	1 sec
t_r	Resource Allocation Slot	200 msec
κ	Interference Distance	200 m
s	Data Size	40MByte
G	Number of Candidate Directions	21
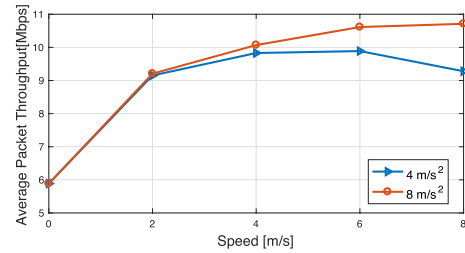
FIGURE 3. The average packet throughput for DBSs with various speeds and two different maximum centripetal accelerations.
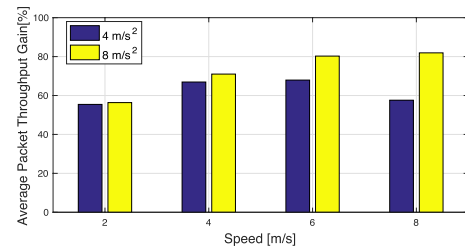
FIGURE 4. The average packet throughput gain for DBSs with various speeds and two different maximum centripetal accelerations.

A. IMPACT OF DBSS' SPEED AND ACCELERATION

In this section, we fixed the number of DBSs to 49. Moreover, the number of users in the area is 245. The DBSs which are following our proposed *GT* algorithm are compared against *HOV* model in terms of various performance metrics.

1) AVERAGE PACKET THROUGHPUT

Figure 3 plots the average packet throughput of the system when DBSs are moving at various speeds, while the speed of "0" represents the *HOV* scenario. From this figure, we can draw the following observations:

- Generally speaking, the average packet throughput of the mobile DBSs becomes larger with a higher speed. Note that considering the working frequency and the maximum speed of 8m/s, the Doppler effect is negligible. Moreover, a higher acceleration generates better results than a lower acceleration.

- Although flying the drone faster may help taking the DBS from one location to another in less amount of time, the higher moving speed reduces the maximum turning angle limiting the possible directions the DBS can move. As a result, by having a low maximum centripetal acceleration the system suffers from lower average packet throughput at higher speed. However, in higher acceleration, drones are able to enjoy both higher speed and higher maneuverability, and the average packet throughput increases by increasing the drones' speed.

- Regardless of the speed and the acceleration, the mobile DBSs moving freely in the network area yield a considerably higher average packet throughput than that of the *HOV* model. The achieved gain of average packet throughput for various speeds and accelerations are plotted in Figure 4. For example, with the current drone
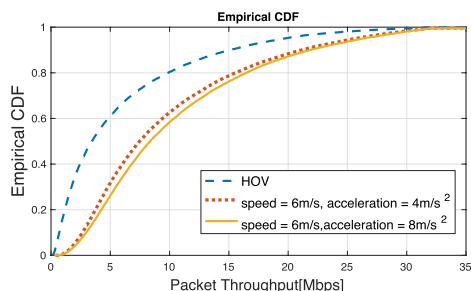
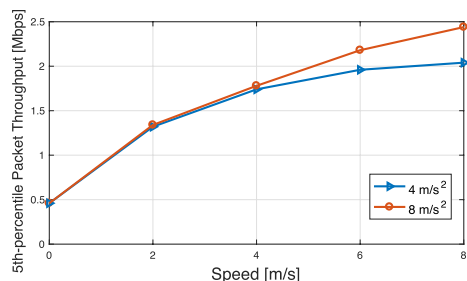**FIGURE 5.** The empirical CDF of packet throughput, having 49 DBSs and 245 users.

FIGURE 6. 5th-percentile packet throughput for DBSs with various speeds and two different accelerations.
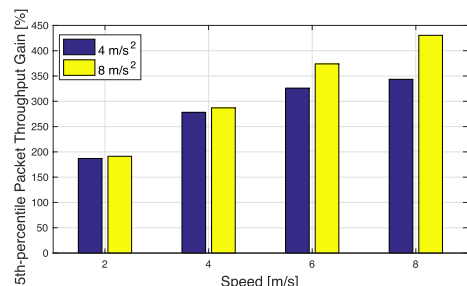

FIGURE 7. 5th-percentile packet throughput gain for DBSs with various speeds and two different accelerations.

technology and the acceleration of $4m/s^2$, a remarkable 67 % gain can be achieved when DBSs are moving at a low speed of 4m/s. By increasing the acceleration to $8m/s^2$, and the speed to 8m/s, an even larger performance gain of 82 % can be obtained.

Moreover, to have a better understanding on the performance gains, we have plotted the empirical CDF of the packet throughput for the *HOV* model with the *GT* algorithm in Figure 5. For the GT algorithm, drones are flying with the speed of 6m/s with two different acceleration of $4m/s^2$ and $8m/s^2$, respectively. This figure shows that the *GT* algorithms noticeably pushes the packet throughput CDF to the right compared to the *HOV* model. Additionally, it can be observed that a higher acceleration has led to a larger packet throughput.

2) 5TH-PERCENTILE PACKET THROUGHPUT
The 5th-percentile packet throughput and the achievable gain are compared to *HOV* model, and plotted in Figure 6 and 7, respectively. From these two figures, we can draw the following observations:

- The 5th-percentile packet throughput improves as the DBSs' speed and acceleration increase.
- According to Figure 7, there is a large performance gain in terms of the 5th-percentile packet throughput, reaching up to 343 % and 430 % improvement with the existing consumer drones (an acceleration of $4m/s^2$) and the future drones (an acceleration of $8m/s^2$), respectively. This is because our algorithm allows drones to move to the vicinity of users, while hovering drones are stationary at pre-defined locations and thus cannot deliver satisfactory QoS to cell-edge users.

We also summarized the 50th-percentile and 95th-percentile packet throughput [in Mbps] along with the achieved gain in Table 2 and Table 3, respectively. Both Table 2 and Table 3 indicate that mobile DBSs following our proposed GT algorithm can achieve a remarkable gain comparing to the scenario where base stations are hovering above fixed locations. Generally speaking, a higher acceleration generates a higher gain as well.

TABLE 2. 50th-percentile packet throughput and the achieved gain.

Speed/Acceleration	$4\ m/s^2$	$8\ m/s^2$
2m/s	6.86 (99.4%)	6.96 (102.3%)
4m/s	7.52 (118.6%)	7.9 (129.6%)
6m/s	7.46 (116.8%)	8.34 (142.4%)
8m/s	6.86 (99.4%)	8.4 (144.1%)

TABLE 3. 95th-percentile packet throughput and the achieved gain.

Speed/Acceleration	$4\ m/s^2$	$8\ m/s^2$
2m/s	24.86 (26.5%)	624.7 (25.7%)
4m/s	25.56 (30.1%)	25.7(31.1%)
6m/s	25.68 (30.7%)	26.2 (33.6%)
8m/s	24.7 (25.7%)	26.4 (34.4%)

3) USER TO DBS DISTANCE
The goal of designing mobility algorithms for DBSs is to reduce the distance between users and the serving BS. Therefore, in this subsection, we show how the DBS-to-user distance reduces with mobile DBSs.

We collected the *ground distance* statistics between any active user and its corresponding DBS during the entire simulation time. Figure 8 shows the average ground distances for the proposed algorithm and the baseline model, where drones are moving at various speeds. The results are plotted for two different accelerations as well, i.e., $4m/s^2$ and $8m/s^2$. According to this figure, there is a substantial reduction in the average user-to-DBS distance, reaching up to 33% and 38% reduction with the existing consumer drones (an acceleration of $4m/s^2$), and the future drones (an acceleration of $8m/s^2$), respectively.

4) PROBABILITY OF LOS
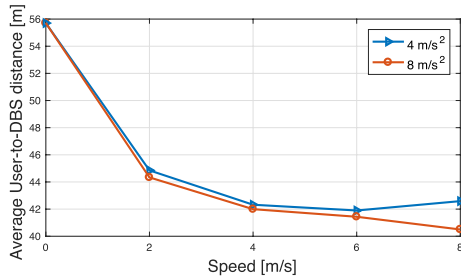Having a LoS link between a user and a DBS will greatly improve the communication performance. In the proposed

FIGURE 8. The average user to DBS ground distance as a function of DBSs' speed and acceleration.
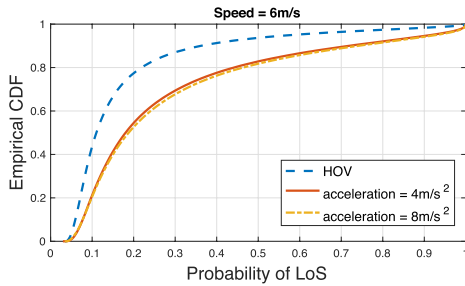

FIGURE 9. Empirical CDF of the probability of LoS connection for the HOV model with the GT algorithm.
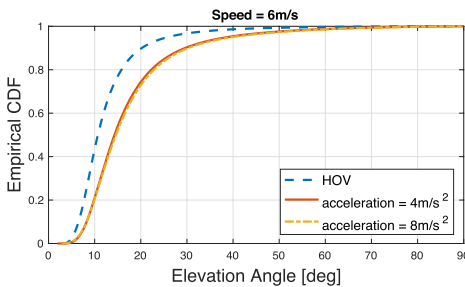

FIGURE 10. Empirical CDF of the elevation angle for GT and HOV.

model, DBSs are adapting themselves in a way to increase the probability of having a LoS link. Figure 9 exhibits the CDF of the probability of LoS for any communication link between active users and their serving DBSs during the simulation time. In this figure, drones are moving at the speed of 6m/s. According to this figure, the proposed *GT* algorithm successfully pushes the CDF rightward compared against the *HOV* scenario. Moreover, it shows that a higher acceleration outperforms a lower one in terms of the probability of having LoS communications. Having a LoS communication depends on the elevation angle of the transmission link. Therefore, in Figure 10 we show the CDF of the elevation angle the for the proposed GT algorithm and the baseline model, where drones are moving at the speed of 6m/s for the GT algorithm, given two different accelerations. Similar to the probability of LoS, the GT algorithm, effectively pushes the elevation angle CDF to the right side. Having larger elevation angles means that the BS has reduced the distance to the user and try to position itself on top of the user's location.
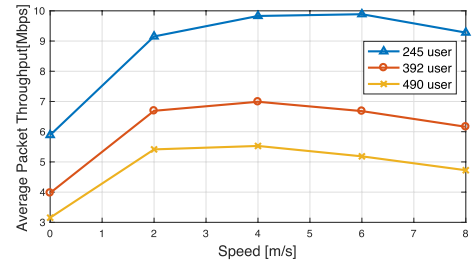

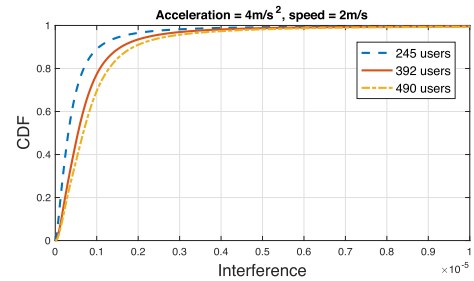**FIGURE 11.** The average packet throughput for different user density.

FIGURE 12. The empirical CDF of interference for different user density.

B. IMPACT OF USER DENSITY

In this section, we change the number of users in the same network area to see how DBSs perform having a different number of users.

Figure 11 illustrates the average packet throughput for the *HOV* model with the *GT* algorithm, when there are 49 DBSs in the network area. Three different user densities are considered in this figure. From Figure 11, the following observations can be drawn:

- Given a fixed number of DBSs, increasing the number of users in the network area decreases the average packet throughput. The reason is that a large number of users have more requests to be served by the DBSs; as a result, each DBS needs to transmit a longer time than the case with a less number of users in the area. More transmissions by DBSs create more interference, and thus reduces the system performance. Such conclusion is corroborated by the results in Figure 12. This figure presents the empirical CDF of interference when DBSs are moving at the speed of 4m/s. According to this figure, having 490 users creates more interference than having 392 and 245 users. Additionally, we summarize the average percentage of transmission time for DBSs during the simulation time in Table 4. This table verifies that the average transmission time for drones increases noticeably as the user density grows. For example, the average transmission time for drones moving at the speed of 2m/s in the *GT* algorithm increases from 41.2 % to 75.9 % as the number of users increases from 245 to 490.

- Regardless of the number of users in the area, the proposed flying DBSs outperforms the baseline HOV model

TABLE 4. Average percentage of transmission time for drones during the simulation time.

Density/Model	HOV	GT(speed = 2m/s)	GT (speed = 8m/s)
245 Users	55.7%	41.2%	38.9%
392 Users	74.6%	64.6%	63.6%
490 Users	82%	75.9%	76.1%
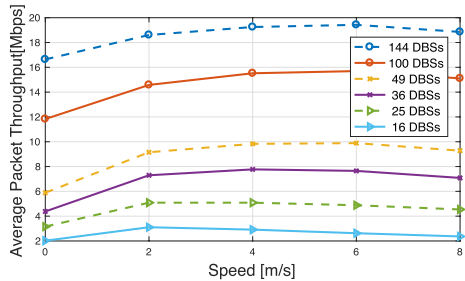
FIGURE 13. Average packet throughput as a function of number of DBSs with 245 users.

FIGURE 14. Variation of associated users to DBSs as a function of number of DBSs with 245 users.
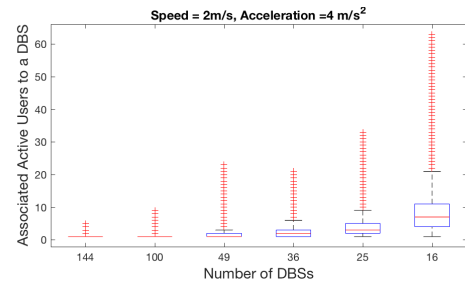

FIGURE 15. Average packet throughput gain as a function of number of DBSs with 245 users.

considerably in term of the average packet throughput. For instance, having DBSs with a speed of merely 2m/s, yields a gain of 68 % and 71 % for a DBS network with 392 and 490 users, respectively.
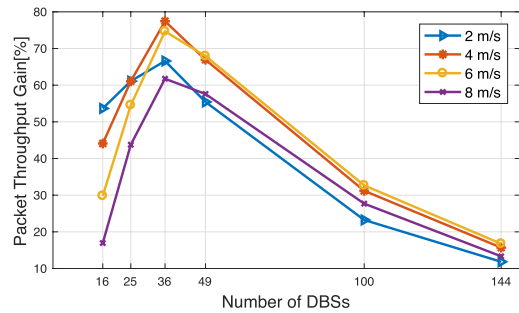
C. IMPACT OF NUMBER OF DBSS

When DBSs and users can move freely in the entire network area, there is no physical constraint on the number of deployed DBSs. As a result, we conduct simulations with different number of DBSs in the area and evaluate the packet throughput. Moreover, the results are compared against the HOV model, where the same number of DBSs are deployed in the network, hovering at the centre of considered grids. We first set the number of users to 245. From Figure 13, the following observations can be drawn:

- The average packet throughput reduces as the number of deployed DBSs decreases in the network. By having a less number of DBSs in the area, each DBS needs to serve a larger number of users; thus the average packet throughput reduces. The variation of the number of active users served by DBSs during the simulation time is plotted in Figure 14. In this figure, the median number of served users is plotted using a red line in a box for each number of DBSs in the area. Moreover, the variations are shown in + symbol in red color. As it can be seen from this figure, there is a possibility of serving 60 users by one DBS in the case of deploying 16 DBSs in the network area. On the other hand, a drone may serve up to 7 users when 144 DBSs are available in the network area.
- Utilizing the mobility features of drones provides an exciting opportunity to reduce the number of required BSs in the network. As shown in Figure 13, having 36 flying DBSs can achieve a similar packet throughput performance to that of 49 fixed hovering DBSs.
- For a given number of DBSs, mobile DBSs following our proposed algorithm can bring a huge improvement in

terms of packet throughput compared to the same number of hovering DBSs. However, the obtained gain could be different depending on the number of available DBSs. To see how the achieved average packet throughput gain varies with various number of DBSs, we plot the gain in Figure 15.

As can be seen from Figure 15, one interesting finding is that the performance gain increases at first, however it wanes when the number of DBSs is larger than 36. This figure indicates that the highest performance gain can be obtained by 36 DBSs in the area. Through dense deployment of DBSs (e.g., 144 DBSs), there is less chance for DBSs to move around. As a result, they cannot provide a high performance gain.

Figure 15 also presents the gains as a function of drones' speed. It indicates that regardless of the speed of drones, the highest performance gain can be achieved by 36 DBSs when there are 245 users in the network area.

To see how the gain varies by the change of the user number, we also plot the achievable gain for variable number of DBSs when there are 392 users in the network area in Figure 16. Interestingly, this figure shows that the optimal number of DBSs to achieve the maximum gain is 49 DBSs, when there are 392 users in the network.

From Figure 15 and Figure 16, it can be concluded that there is an optimal number of DBSs to achieve the maximum gain in the network area. However, such optimal number depends on the user density. It shows that with a higher user density, a higher DBS density is needed to achieve the maximum gain. The reason is that with too few DBSs the
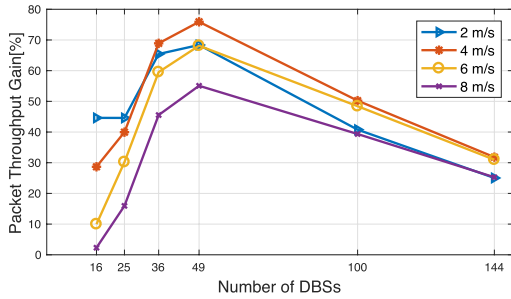
FIGURE 16. Average packet throughput gain as a function of number of DBSs with 392 users.
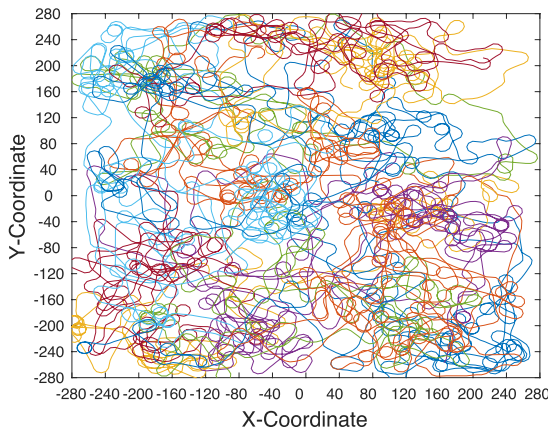

FIGURE 17. Trajectory of 16 DBSs in the network area, moving at the speed of 6m/s and acceleration of $4m/s^2$.

FIGURE 18. The empirical CDF of DBS-to-DBS distance.

gain of DBS mobility is limited because of the large BS-to-user distance. On the other hand, with too many DBSs the baseline scheme of hovering is already good enough. Therefore, the movement of drones does not make a large difference. The relation between the optimal DBS number and the user density is left for future work.

We also provide the moving trajectory of DBSs in the entire network area during the simulation time to see how they chase the users in the network. According to Figure 17, mobile DBSs can leverage their mobility in order to cover the entire area and provide high quality services for the users even if the density is low.

D. THE DBSS COLLISION ISSUE

Note that when drones are moving freely at the same height, they may collide with each other. To study the probability of collision, we analyze the DBS-to-DBS distance during the simulation time. Figure 18 illustrates the CDF of such DBS-to-DBS distance for the free movement models. As can be seen from this figure, the intelligent movement of drones maintains a comfortable distance among the DBSs. The intuition is that in the proposed algorithm, each DBS tends to be closer to its serving users, and farther away from interfering DBSs. Therefore, the possibility of having two drones flying in close proximity is extremely low, which helps to prevent drones coming too close to each other. As shown
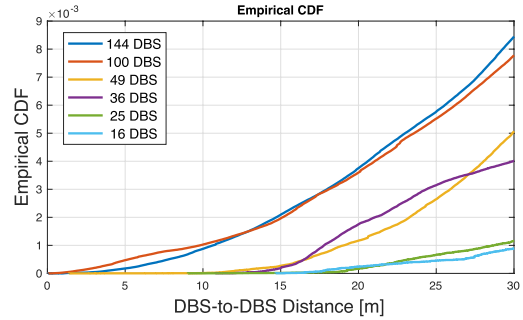
in Figure 18, the probability that the DBS-to-DBS distance is less than 10m, is well below 10^{-3} even for dense DBSs deployment.

VII. CONCLUSION

In this paper, we considered a macro hotspot scenario, where both flying DBSs and users can move freely in the entire network area. The flying DBSs serve as many users as they can based on the received signal strength. We shows that by freeing up the DBSs and letting them cruise in the network, a significantly large system throughput can be achieved. This enormous performance is the result of an intelligent and effective control mobility algorithm and a practical user association scheme. Moreover, by allowing DBSs to move freely, the opportunity to deploy a less number of DBSs becomes promising. The performance impact of the DBS and user densities have also been studied in this paper.

REFERENCES

[1] I. Bekmezci, O. K. Sahingoz, and Ş. Temel, "Flying ad-hoc networks (FANETs): A survey," *Ad Hoc Netw.*, vol. 11, no. 3, pp. 1254–1270, 2013.

[2] A. Al-Hourani, S. Kandeepan, and S. Lardner, "Optimal LAP altitude for maximum coverage," *IEEE Wireless Commun. Lett.*, vol. 3, no. 6, pp. 569–572, Dec. 2014.

[3] K. Gomez, A. Hourani, L. Goratti, R. Riggio, S. Kandeepan, and I. Bucaille, "Capacity evaluation of aerial LTE base-stations for public safety communications," in *Proc. Eur. Conf. Netw. Commun. (EuCNC)*, Jun. 2015, pp. 133–138.

[4] A. Al-Hourani, S. Kandeepan, and A. Jamalipour, "Modeling air-to-ground path loss for low altitude platforms in urban environments," in *Proc. IEEE Global Commun. Conf. (GLOBECOM)*, Austin, TX, USA, Dec. 2014, pp. 2898–2904.

[5] D. G. Cileo, N. Sharma, and M. Magarini, "Coverage, capacity and interference analysis for an aerial base station in different environments," in *Proc. Int. Symp. Wireless Commun. Syst. (ISWCS)*, Aug. 2017, pp. 281–286.

[6] M. Mozaffari, W. Saad, M. Bennis, and M. Debbah, "Optimal transport theory for power-efficient deployment of unmanned aerial vehicles," in *Proc. IEEE Int. Conf. Commun. (ICC)*, May 2016, pp. 1–6.

[7] R. I. Bor-Yaliniz, A. El-Keyi, and H. Yanikomeroglu, "Efficient 3D placement of an aerial base station in next generation cellular networks," in *Proc. IEEE ICC*, May 2016, pp. 1–5.

[8] D. Takaishi, H. Nishiyama, N. Kato, and R. Miura, "A dynamic trajectory control algorithm for improving the probability of end-to-end link connection in unmanned aerial vehicle networks," in *Proc. Int. Conf. Next-Generat. Satellite Netw. Commun. Syst.*, May 2014, pp. 94–105.

[9] A. E. A. A. Abdulla, Z. M. Fadlullah, H. Nishiyama, N. Kato, F. Ono, and R. Miura, "An optimal data collection technique for improved utility in UAS-aided networks," in *Proc. IEEE INFOCOM*, Apr./May 2014, pp. 736–744.

[10] M. Zhu, Y. Chen, Z. Cai, and M. Xu, "Using unmanned aerial vehicle chain to improve link capacity of two mobile nodes," in *Proc. IEEE Int. Conf. Mechatronics Autom. (ICMA)*, Aug. 2015, pp. 494–499.

[11] F. Jiang and A. L. Swindlehurst, "Optimization of UAV heading for the ground-to-air uplink," *IEEE J. Sel. Areas Commun.*, vol. 30, no. 5, pp. 993–1005, Jun. 2012.

[12] Y. Zeng *et al.*, "Throughput maximization for UAV-enabled mobile relaying systems," *IEEE Trans. Commun.*, vol. 64, no. 12, pp. 4983–4996, Dec. 2016.

[13] A. Fotouhi, M. Ding, and M. Hassan. (Jun. 2017). "DroneCells: Improving 5G spectral efficiency using drone-mounted flying base stations." [Online]. Available: https://arxiv.org/abs/1707.02041

[14] M. Shanmugavel, A. Tsourdos, B. White, and R. Żbikowski, "Co-operative path planning of multiple UAVs using dubins paths with clothoid arcs," *Control Eng. Pract.*, vol. 18, no. 9, pp. 1084–1092, 2010.

[15] X. Lin, R. K. Ganti, P. J. Fleming, and J. G. Andrews, "Towards understanding the fundamentals of mobility in cellular networks," *IEEE Trans. Wireless Commun.*, vol. 12, no. 4, pp. 1686–1698, Apr. 2013.

[16] X. Ge, J. Ye, Y. Yang, and Q. Li, "User mobility evaluation for 5G small cell networks based on individual mobility model," *IEEE J. Sel. Areas Commun.*, vol. 34, no. 3, pp. 528–541, Mar. 2016.

[17] A. Merwaday and I. Guvenc, "Handover count based velocity estimation and mobility state detection in dense HetNets," *IEEE Trans. Wireless Commun.*, vol. 15, no. 7, pp. 4673–4688, Jul. 2016.

[18] *further Enhancements to LTE Time Division Duplex for Downlink-Uplink Interference Management and Traffic Adaptation*, document 3GPP TR 36.828, 3GPP, 2012.

[19] *Further Advancements for E-UTRA Physical Layer Aspects Release 9*, document 3GPP TR 36.814 version 9.0.0, 3GPP, 2010.

[20] C. S. Turner. (2012). *Johnson-Nyquist Noise*. [Online]. Available: http://www.claysturner.com/dsp/Johnson-NyquistNoise

[21] J. G. Proakis, *Digital Communications*, 4th ed. New York, NY, USA: McGraw-Hill, 2000.

[22] G. Avanzini, G. de Matteis, and L. M. de Socio, "Analysis of aircraft agility on maximum performance maneuvers," *J. Aircraft*, vol. 35, no. 4, pp. 529–535, 1998.

[23] *Requirements for Further Advancements for Evolved Universal Terrestrial Radio Access (E-UTRA) (LTE-Advanced Release 14)*, document 3GPP TR 36.913, 3GPP, 2017.

[24] A. Fotouhi, M. Ding, and M. Hassan, "Understanding autonomous drone maneuverability for Internet of Things applications," in *Proc. IEEE WoW-MoM Workshops*, Jun. 2017, pp. 1–6.

[25] M. Ding and D. L. Perez, "Please lower small cell antenna heights in 5G," in *Proc. IEEE GLOBECOM*, Dec. 2016, pp. 1–6.

MING DING (M'12–SM'17) received the B.S. and M.S. degrees (Hons.) in electronics engineering and the Ph.D. degree in signal and information processing from Shanghai Jiao Tong University, Shanghai, China, in 2004, 2007, and 2011, respectively. From 2007 to 2014, he was with Sharp Laboratories of China, Shanghai, as a Researcher/Senior Researcher/ Principal Researcher. He also served as the Algorithm Design Director and the Programming Director for a system-level simulator of future telecommunication networks with Sharp Laboratories of China for over seven years. He is currently a Senior Research Scientist with Data61, CSIRO, Sydney, NSW, Australia. He has authored over 70 papers in the IEEE journals and conferences, all in recognized venues, and about 20 3GPP standardization contributions, as well as a Springer book *Multi-point Cooperative Communication Systems: Theory and Applications*. He holds 14 U.S. patents and co-invented another over 100 patents on 4G/5G technologies in CN, JP, and EU. For his inventions and publications, he was a recipient of the President's Award of Sharp Laboratories of China in 2012, and served as one of the key members in the 4G/5G standardization team when it honored as the Sharp Company Best Team: LTE 2014 Standardization Patent Portfolio in 2014. He was the Lead Speaker of the industrial presentation on unmanned aerial vehicles in the IEEE Globecom 2017, which received the Most Attended Industry Program in the conference. He also received the Exemplary Reviewer for the IEEE TRANSACTIONS ON WIRELESS COMMUNICATIONS in 2017. He is currently an Editor of the IEEE TRANSACTIONS ON WIRELESS COMMUNICATIONS. He is or has been the Guest Editor/Co-Chair/Co-Tutor/TPC Member of the several IEEE top-tier journals/conferences, such as, the IEEE JOURNAL ON SELECTED AREAS IN COMMUNICATIONS, the *IEEE Communications Magazine*, and the IEEE GLOBECOM Workshops.

AZADE FOTOUHI received the B.S. degree (Hons.) in computer engineering from the Isfahan University of Technology in 2008, the M.S. degree (Hons.) in computer engineering from the Amirkabir University of Technology, Iran, in 2011, and the Ph.D. degree in computer science and engineering from the University of New South Wales, Australia, in 2017. She was a Post-Doctoral Researcher with Data61|CSIRO until 2018. Her research interests include mobile networks, UAVs, machine learning, and IoT. She was a recipient of the International Postgraduate Research Scholarships, and Data61|CSIRO Research Project Award during her Ph.D.

MAHBUB HASSAN (M'91–SM'00) received the M.Sc. degree in computer science from the University of Victoria, Victoria, BC, Canada, and the Ph.D. degree in computer science from Monash University, Australia. He was a Visiting Professor with Washington University in St. Louis, Osaka University, and the University of Nantes. He is currently a Full Professor with the School of Computer Science and Engineering, University of New South Wales, Sydney, Australia. His current research interests include UAV networking, Internet of Things, pervasive and wearable computing, and millimeter wave networking. He was one of the presenters of the industrial tutorial Drone Base Stations: Opportunities and Challenges Toward a Truly Wireless Wireless Network which received the Most Attended Industry Program Award at IEEE GLOBECOM 2017. He was the Guest Editor for the IEEE NETWORK, the *IEEE Communications Magazine*, and the IEEE TRANSACTIONS ON MULTIMEDIA, and an Area Editor for *Computer Communications*. He is currently an Editor of the IEEE COMMUNICATIONS SURVEYS AND TUTORIAL. He was a Distinguished Lecturer of the IEEE Communications Society from 2013 to 2016.

• • •